

Structural quality of $\text{Hg}_{1-x}\text{Cd}_x\text{Te}$: Equilibrium point defects

C. G. Morgan-Pond*

Riverside Research Institute, 330 West 42nd Street, New York, New York 10036

R. Raghavan[†]

*Research and Development Division, Lockheed Missiles and Space Company, Inc.,
3251 Hanover Street, 0/95-43 Building 202,
Palo Alto, California 94304*

(Received 19 October 1984)

The Phillips–Van Vechten dielectric theory for estimating enthalpies of defect formation and defect concentrations is applied to CdTe and narrow-gap $\text{Hg}_{1-x}\text{Cd}_x\text{Te}$ ($\text{Hg}_{0.8}\text{Cd}_{0.2}\text{Te}$). It is found that favorable ionization levels in CdTe lead to large charged native defect densities ($\sim 10^{18}/\text{cm}^3$; $\sim 4 \times 10^{17}/\text{cm}^3$ net at 1365 K), which can condense into extended defects, such as dislocations and Te inclusions at lower temperatures. Intentional incorporation of small amounts of impurities or use of substitutional alloys, such as $\text{Cd}_{0.96}\text{Zn}_{0.04}\text{Te}$, has often been suggested as a means of improving the quality of CdTe crystals, and addition of Zn or Mn has also been suggested as a means of reducing cation-vacancy concentrations in Hg-rich $\text{Hg}_{1-x}\text{Cd}_x\text{Te}$. It is shown that equilibrium concentrations of native point defects are not reduced substantially by adding small amounts of other elements either to CdTe or to Hg-rich $\text{Hg}_{1-x}\text{Cd}_x\text{Te}$, although macroscopic and nonequilibrium phenomena, such as formation of dislocations, may be significantly affected. Increasing metallicity upon addition of Hg to the alloy and the volatility of elemental Hg lead to preferential loss of Hg from $\text{Hg}_{1-x}\text{Cd}_x\text{Te}$, which must be balanced, in equilibrium, by a larger proportion of Hg in the external phase. The observed strong *p*-type character of $\text{Hg}_{0.8}\text{Cd}_{0.2}\text{Te}$, in contrast to the strongly compensated character of CdTe at high temperature, results both from this and from highly favorable cation-vacancy ionization levels.

I. INTRODUCTION

The defect chemistry of even the most thoroughly studied semiconductors, such as Si, is not completely understood. Deep levels and recombination centers observed at room temperature and below are generally complexes, and the difficulty of doing experiments at elevated temperatures generally precludes the gathering of much data on the simple defects which should dominate at these temperatures in equilibrium. In addition, kinetic effects and nonequilibrium processes often determine the dominant characteristics of semiconductors grown by standard production methods.

Defect problems are particularly severe in CdTe and Hg-rich $\text{Hg}_{1-x}\text{Cd}_x\text{Te}$, which have failed to realize the promise of their potential electrical and optical performance, due to structural quality limitations. Native point defects (vacancies, interstitials), extended defects (dislocations, precipitates, grain boundaries), and defects involving impurities are numerous in CdTe and $\text{Hg}_{1-x}\text{Cd}_x\text{Te}$, and tend to control the electronic properties of these materials, producing changes in behavior over time and making it difficult to obtain the desired behavior with doping. Although it is not sufficient to consider point-defect formation alone, equilibrium concentrations of these defects should be dominant during high-temperature growth at the melting point, so they form a natural starting point for discussion of later condensation of excess anions or cations into complexes or extended defects. A subsequent

paper will discuss the effects of complexes with added donors (In) and possible effects of clustering of isovalent substituents (Zn) on the formation of extended defects, and the sensitivity of diffusion barriers to the addition of small amounts of other elements. In this paper we concentrate on equilibrium densities of native point defects under various growth and annealing conditions for CdTe and $\text{Hg}_{0.8}\text{Cd}_{0.2}\text{Te}$.

In Sec. II the main features of the dielectric theory and the modifications needed to apply it to the $\text{Hg}_{1-x}\text{Cd}_x\text{Te}$ system are reviewed, along with the thermodynamics needed to compute the defect densities in equilibrium. Section III contains our results for CdTe, and Sec. IV, those for $\text{Hg}_{0.8}\text{Cd}_{0.2}\text{Te}$. Our conclusions are summarized in Sec. V.

II. SUMMARY OF THEORY AND PARAMETERS

A. The dielectric approach to defect chemistry

The dielectric theory of Phillips and Van Vechten,¹ in contrast to the models discussed by Harrison,² is not universal. This means, in particular, that the basic parameters of the theory depend on the crystal structure considered. As used here, the dielectric theory is restricted to tetrahedrally bonded (*sp*³) crystals. Indeed, it begins to develop important flaws in the regimes where competi-

tion from octahedral coordination (due to s - d and p - d mixing) become strong. This is so in the mercury-rich end of the alloy. It would be valuable to have a more complete development of the theory and its basic parameters for such cases, but such developments are relegated to future work. To compensate for its lack of universality, the dielectric theory is a valuable semiempirical theory that leads directly to thermodynamic quantities of interest.

The reference state of the dielectric theory is a free-electron metal. This is useful since most of the liquids considered here (though not Te) are metals, albeit not "ideal" free-electron fluids. All energies, unless explicitly stated, are referred to this state, and bond energies, etc. refer to the crystal as a whole and not, as in a local tight-binding picture, to a specific atom and its nearest neighbors.

The dielectric theory has been used successfully to calculate enthalpies of formation of neutral vacancies in Si, Ge, and various zinc-blende and wurtzite crystals.^{3,4} We use this theory for neutral-vacancy-formation enthalpies. We use experimentally identified low-temperature vacancy ionization levels, where available, together with the temperature dependence for the ionization levels of localized states derived by Van Vechten and Thurmond,⁵ following Heine and Henry.⁶

Interstitials seem to be less well understood than vacancies, partly because interstitials often tend not to be simple interstitials, but semibonded, which disturbs the bonding structure in their vicinity. We find that Van Vechten's method¹ gives excessive interstitial formation energies for these very ionic alloys, in particular, for Te interstitials. Results of self-diffusion of Te in CdTe, as well as Se and Te in CdSe, ZnSe, and ZnTe, indicate that Te and other chalcogen interstitials are numerous and sufficiently mobile to dominate the self-diffusion properties under a wide variety of conditions.⁷ For crystals such as CdTe, with large lattice constants, relatively open zinc-blende structure, and relatively nondirectional ionic bonds, it may cost little energy to form a semibonded neutral interstitial.

Favorable ionization levels may then promote the creation of charged interstitials with a closed-shell configuration (I_{Cd}^{+2} or I_{Te}^{-2}), which would not be bonded to the rest of the crystal, and could therefore be highly mobile. We use the results of Huntington and Seitz^{8,9} to estimate plausible values for the enthalpy of creation of a semibonded neutral interstitial, and treat the ionization levels for interstitials in the same way as described for vacancies.

Enthalpies of formation for antisite defects¹⁰ are prohibitively high in such ionic compounds as CdTe and $\text{Hg}_{1-x}\text{Cd}_x\text{Te}$. Therefore, we consider only cation and anion self-interstitials and vacancies. In Table I we summarize the principal dielectric theory parameters¹ needed to describe reactions involving these defects, and we discuss these parameters and the principal uncertainties in their values in the following sections.

B. Initial assumptions and parameters

In the dielectric theory, bonding energies are described by a covalent radius and by scaling forms for energies

which are functions of that radius. The tetrahedral covalent radii for the cation and anion (r_C, r_A) listed in Table I were obtained by using the lattice constant, $a(T)$, as a function of temperature T , to take into account thermal expansion, and the standard Phillips-Van Vechten core and valence radii r_c and r_v , which are functions of the atomic number, Z .¹¹ (The average cation radius for the alloy $\text{Hg}_{0.8}\text{Cd}_{0.2}\text{Te}$ was obtained from the virtual-crystal approximation. Since the natural radius $r_C = 1.405 \text{ \AA}$ for Cd and is 1.461 \AA for Hg at 300 K,¹¹ a change in the method of averaging should produce less than a 4% difference in the average r_C and bond energies calculated from it.) Although more sophisticated coordinates (separate radii for each angular-momentum state) have since been suggested and used,¹² the covalent radii employed work well when compared with experiment, until we reach the Hg row. The principal difficulty in our applications is that Hg is a strong exception to the scaling formulas. This is shown by the discrepancy (1.45 versus 1.403 \AA) between the natural (scaled) and actual r_C in $\text{Hg}_{0.8}\text{Cd}_{0.2}\text{Te}$. The reason for this is discussed in Ref. 11, and involves the strong mixing of the d states with the bonding electrons and consequent perturbation of the tetrahedral bonding configuration by an octahedral one. This constitutes the principal theoretical shortcoming in our calculations, but an extension of the dielectric theory in the required direction is a subject for future research.

The ionic¹³ and covalent¹⁴ contributions to the bond energy, C and E_h , are calculated using the screening wave vector, k_s , appropriate for a uniform electron gas of the same average density as in the alloy, and the natural cation radius. This is equivalent to assuming that the fractional ionic character is unchanged and the average Penn gap E_g is not greatly changed by the compression induced by d -state mixing. The ionicity C is due to a screened Coulomb interaction between anion and cation.

ΔE_m is the energy of the Penn model¹⁵ of the semiconductor relative to the metallic state, and \bar{E}_F is the free-electron-gas Fermi level at the average density of electrons appropriate for the semiconductor.

The metallicity \mathcal{D} is calculated from optical features.¹⁴ (The metallicity is unfortunately named, since the limits $\mathcal{D} = 0$ and 1 correspond to purely metallic and purely nonmetallic bonding, respectively.) \mathcal{D} is calculated from the optical gaps E_i^{av} averaged over the spin-orbit splitting.

For E_0^{av} of CdTe, and for all the gaps of the Hg-rich compound, we use the experimental gaps¹⁶⁻¹⁸ at 300 K as a starting point. There is considerably more uncertainty in the value used here for E_2^{av} (300 K) than for the other gaps in $\text{Hg}_{0.8}\text{Cd}_{0.2}\text{Te}$, as there is considerable disagreement over the assignment of the optical features in the E_2 region to precise parts of phase space, and whether these features come from the same parts of phase space for different alloys.¹⁹ We found a reasonable match only for E_{2A} ; however, different choices from among all the cited E_2 gaps in $\text{Hg}_{1-x}\text{Cd}_x\text{Te}$ give similar final results. For CdTe, where scaling formulas for the E_i^{av} work well, we use them to get the appropriate zero-temperature gaps, E_1^{av} (0 K), and E_2^{av} (0 K), as functions of lattice constant a .²⁰

The question of the temperature dependence of the gaps

TABLE I. Parameters from the dielectric theory (see also explanation in text).

Symbol	Description	Defining relations												
r_C, r_A	Natural covalent radii of cation, anion	$r(Z, T) = \max(r_V(Z), r_V(Z) + \{r_c(Z) - 0.4 r_V(Z)\}) \times a(T)/a(300 \text{ K})$ $a = \text{lattice constant}$												
k_s	Screening wave vector	$k_s^2 = 4k_F/\pi a_B; k_F^3 = 3\pi^2 N/V$												
C	Ionic energy gap	$C = 1.5 \left[\frac{Z_A e^2}{r_A} - \frac{Z_C e^2}{r_C} \right] e^{-k_s(r_A + r_C)/2}$ $Z_A, Z_C = \text{anion, cation valence}$												
E_h	Covalent gap	$E_h = 4.8(a/a_{\text{Si}})^{-2.48} \text{ eV}$ $a_{\text{Si}} = 5.43 \text{ \AA}$												
E_g	Penn gap	$E_g^2 = C^2 + E_h^2$												
ΔE_m	Energy relative to metal per atom pair	$\Delta E_m = -\tilde{E}_F \{3B^2(1 + \ln[B/2]) - 4B^3\}$ $B = E_g/4\tilde{E}_F; \tilde{E}_F = \text{free-electron Fermi energy per } e^-$												
\mathcal{D}	Metallicity	$\mathcal{D} = 1 - b \left[\frac{2E_2^{\text{av}}}{E_0^{\text{av}} + E_1^{\text{av}}} \right]^2 + c \left[\frac{E_0^{\text{av}} + E_1^{\text{av}}}{2E_2^{\text{av}}} \right]^2$ $b = 0.0467, c = 0.0875$												
E_i^{av}	Spin-orbit averaged optical gaps	Expt: $E_0^{\text{av}}(300 \text{ K}) = E_0(300 \text{ K}) + \frac{1}{3}\Delta_0(300 \text{ K})$ $E_1^{\text{av}}(300 \text{ K}) = E_1(300 \text{ K}) + \frac{1}{2}\Delta_1(300 \text{ K})$ $E_2^{\text{av}}(300 \text{ K}) = \frac{1}{2}E_{2A}(300 \text{ K}) + E_{2B}(300 \text{ K})$ Theory: $E_i^{\text{av}}(0) = E_{h,i} - \Delta E_i(D_{\text{av}} - 1) \left[1 + \frac{C}{E_{h,i}} \right]^2$ D_{av} measures effective plasma frequency ($D_{\text{av}} \neq \mathcal{D}$) $D_{\text{av}} = 1.3$ for CdTe												
$E_{h,i}$	Covalent gaps	$E_{h,0} = 4.1(a/a_{\text{Si}})^{-2.75} \text{ eV}$ $E_{h,1} = 3.6(a/a_{\text{Si}})^{-2.22} \text{ eV}$ $E_{h,2} = 4.5(a/a_{\text{Si}})^{-2.38} \text{ eV}$												
ΔE_i	Measures effect of d -state mixing on optical gaps	$\Delta E_i = S_i \left[\frac{a}{a_{\text{Si}}} \right]^{-t_i}$ <table style="margin-left: auto; margin-right: auto;"> <tr> <td>i</td> <td>S_i</td> <td>t_i</td> </tr> <tr> <td>0</td> <td>12.8</td> <td>5.07</td> </tr> <tr> <td>1</td> <td>14.97</td> <td>4.97</td> </tr> <tr> <td>2</td> <td>0</td> <td></td> </tr> </table>	i	S_i	t_i	0	12.8	5.07	1	14.97	4.97	2	0	
i	S_i	t_i												
0	12.8	5.07												
1	14.97	4.97												
2	0													
ΔH_m	Surface enthalpy for cation and anion (C, A) vacancies	$\Delta H_{m,C} = (1.9 \text{ eV})[r_C/(1.405 \text{ \AA})]^2/[a/(6.489 \text{ \AA})]^2 \cdot 5H^*$ $\Delta H_{m,A} = (1.9 \text{ eV})[r_A/(1.405 \text{ \AA})]^2/[a/(6.489 \text{ \AA})]^2 \cdot 5H^*$												
$4E_b$	Bond energy per atom pair	$4E_b = \mathcal{D} \Delta E_m$												

TABLE I. (Continued).

Symbol	Reference	Value at 300 K for CdTe	Value at ^a 1365 K for CdTe	Value at 300 K for Hg _{0.8} Cd _{0.2} Te	Value at ^a 825 K for Hg _{0.8} Cd _{0.2} Te
r_C, r_A	11, Eqs. (3.1)–(3.4)	Both 1.405 Å	Both 1.414 Å	Cation 1.450 Å 1.403 Å (natural) (actual) Anion 1.405 Å	Cation 1.454 Å 1.407 Å (natural) (actual) Anion 1.409 Å
k_s	13, Eqs. (4.3), (4.4)	1.910 Å ⁻¹	1.904 Å ⁻¹	1.912 Å ⁻¹	1.909 Å ⁻¹
C	13, Eq. (4.5)	4.194 eV	4.132 eV	4.067 eV	4.037 eV
E_h	14, Eq. (2.3)	3.094 eV	3.045 eV	2.966 eV	2.943 eV
E_g	13, Eq. (1.5)	5.212 eV	5.133 eV	5.034 eV	4.996 eV
ΔE_m	14, Eq. (4.3)	1.046 eV	1.028 eV	0.987 eV	0.9797 eV
\mathcal{D}	14, Eq. (4.6)	0.850	0.812	0.484	0.504
E_i^{av}	16, 17, 22, 21, 25	1.794 eV	1.443 eV	0.509 eV	0.640 eV
	16			2.595 eV	2.414 eV
	18			5.200 eV	5.016 eV
	20, Eq. (3.7)	$E_1^{\text{av}} = 3.594$ eV $E_2^{\text{av}} = 5.190$ eV	$E_1^{\text{av}} = 3.113$ eV $E_2^{\text{av}} = 4.801$ eV		
$E_{h,i}$	20, Eq. (3.2) and Table II	2.519 eV 2.430 eV 2.951 eV	2.476 eV 2.396 eV 2.907 eV		
ΔE_i	20, Eq. (3.2) and Table II	5.215 eV 2.064 eV 0.0 eV	5.050 eV 1.999 eV 0.0 eV		
ΔH_m	4, Eqs. (8), (17) 26, Eq. (2)	1.905 eV (both)	1.899 eV (both)	1.295 eV (cation) 1.300 eV (anion)	1.293 eV (cation) 1.298 eV (anion)
$4E_b$	14, Eq. (4.5)	0.889 eV	0.835 eV	0.478 eV	0.494 eV

^aThese are typical temperatures of growth for liquid-phase methods.

is an important one, since we wish to calculate defect densities at temperatures well above 300 K. We scale the low-temperature values of E_1^{av} and E_2^{av} by a Debye-Waller factor,

$$E_i^{\text{av}}(T)/E_i^{\text{av}}(0) = e^{-A_i T/T_{\text{FS}}},$$

where $e^{-A_1} = 0.828$, $e^{-A_2} = 0.91$, and T_{FS} is the fusion temperature for the semiconductor.¹⁴

For the fundamental gap E_0 , and for E_0^{av} , we use the temperature dependence measured from 77 to 300 K: $dE_0/dT = -0.00033$ eV/K for CdTe,²¹ and $+0.00025$ eV/K for Hg_{0.8}Cd_{0.2}Te.^{17,22} The experimental temperature dependence of E_0 for CdTe is quite similar to that

given by a Debye-Waller factor. For Hg_{0.8}Cd_{0.2}Te, this is not so, at least at low temperatures, since the fundamental gap of Hg_{1-x}Cd_xTe, for $x < 0.5$, increases with temperature for $0 < T < 300$ K. In a division of the temperature dependence of the gap into Debye-Waller, intraband, and interband terms, the last two usually tend to cancel, as discussed by Heine and van Vechten.²³ This is not true for Hg-rich Hg_{1-x}Cd_xTe below 300 K, where the only term that favors an increase of the gap with temperature, the interband term, dominates. This probably arises from a selection rule that forbids the mixing of states from a single band by the lattice deformation potential. This selection rule should become increasingly inoperable at

higher temperatures, so that as the temperature approaches the melting temperature, the band gap of Hg-rich $\text{Hg}_{1-x}\text{Cd}_x\text{Te}$ should increase more slowly, and then begin to decrease. In fact, there appears to be a higher concentration of intrinsic carriers in $\text{Hg}_{0.8}\text{Cd}_{0.2}\text{Te}$ at annealing temperatures of 700–800 K than is given by our simple assumptions,²⁴ which is probably due to this change in the temperature dependence of the fundamental gap as well as to nonparabolicity of the conduction and valence bands. The high concentration of intrinsic carriers gives rise to an observed linear dependence of total equilibrium cation-vacancy concentration on the inverse of the Hg pressure up to concentrations of 10^{17} – $10^{18}/\text{cm}^3$, while the equilibrium cation-vacancy concentrations that we calculate begin to saturate and deviate from a pure linear dependence at lower levels. Improved understanding of the behavior of E_0 and the effective hole and electron masses at high temperatures is therefore suggested as a possible means of improving these studies significantly for materials with an anomalous E_0 dependence at low temperatures, such as $\text{Hg}_{0.8}\text{Cd}_{0.2}\text{Te}$.

ΔH_m is the enthalpy of surface formation around one vacant site in a metal of the same average electron density as the semiconductor. As discussed by Van Vechten,⁴ this is given by the surface tension of a free-electron gas and the surface area surrounding the site. The expression for the surface tension of a free-electron gas was obtained by Schmit and Lucas.²⁵

For $\text{Hg}_{0.8}\text{Cd}_{0.2}\text{Te}$, there is a larger correction for relaxation of the atoms surrounding a vacant site than for CdTe because of the compression of the Hg. We assume that it takes very little energy to vary the Hg radius between its natural, or scaled value, and its actual value in the crystal. This assumption is supported by estimates which show that the bulk modulus for the alloy would be small at the natural radius.²⁶ If we estimate the volume which would be occupied by an anion vacancy, we must take into account the volume reduction due to expansion of the neighboring Hg. We may estimate this effect by assuming that the Hg atoms which are in nearest-neighbor positions [$4(1-x)$ atoms, on the average] will expand to their natural radii, while Hg's in more distant shells will remain completely compressed. Since the measured volume per cation and per anion site in the crystal are nearly equal, we can write the volume reduction of the anion vacancy as

$$\Delta V = 4(1-x)[(1.04)^3 - 1]V$$

in terms of the volume per site, V . The surface area of the vacancy will then be reduced by a factor of $H' = (1 - \Delta V/V)^{2/3}$. In addition, the surface energy per unit area for creation of this surface will be reduced because the average electron density near the surface corresponds to the natural and not the actual lattice constant. We assume that this relaxation changes ΔH_m for neutral cation vacancies in the same proportion as for anion vacancies, although relaxation effects are harder to estimate for cation vacancies, which have twelve second-nearest-neighbor instead of four nearest-neighbor cations. These correction factors are included in $H^* = H'(a_{\text{nat}}/a)^{2.5}$, in Table I. $H^* = 1$ for CdTe.

E_b is the bonding energy (per covalent bond) of the semiconductor relative to a metal of the same electron density.

The above list of parameters describes some of the important properties of the crystal and quantifies the concepts of ionicity and metallicity. What results is a convenient description of some gross features of the charge distribution in the crystal. We now describe the additional theory needed in a description of the formation of defects in a crystal.

C. Native-defect-formation energies

We shall assume throughout most of this discussion that the only point defects of importance are cation and anion vacancies and interstitials, all of which may be neutral, singly ionized, or doubly ionized. In a highly ionic compound such as $\text{Hg}_{1-x}\text{Cd}_x\text{Te}$, there is no ambiguity about the charge states of these defects: cation vacancies and anion interstitials are neutral or negatively charged, while anion vacancies and cation interstitials are neutral or positively charged. Since the ionicity $f_i \equiv C^2/E_g^2$ is a direct measure of charge transfer in the crystal bonds, and since f_i is large for these materials, we expect vacancies to exist predominantly in an ionized state. Interstitials are also expected to be predominantly ionized, since the dielectric constant is large in these materials, so the charge can be well screened. These expectations are confirmed in the quantitative calculations of equilibrium defect densities below.

The quantities needed for the description of nonin-

TABLE II. Steps in cation-vacancy formation (solid equilibrium).

Step	$\Delta G_S = \Delta G_1 + \Delta G_2 + \Delta G_3 + \Delta G_4 = \Delta H(V_c^x) + k_B T \ln[N_V(1-x)/3N]$ Change in Gibbs free energy (ΔG)
(1) crystal(N) \rightarrow metal(N)	$N_b E_b$
(2) metal(N) \rightarrow metal(N) + cavity	$\Delta H_m + k_B T \ln[N_V(1-x)/N] + P_{\text{ext}} \Delta V_s$
(3) metal(N) \rightarrow cavity \rightarrow crystal(N) + cavity	$-(N_b - 2)E_b$
(4) Jahn-Teller distortion of cavity	$-k_B T \ln 3$

interacting point defects, which may be expressed in terms of the parameters defined in Table I, are (1) the neutral-vacancy-formation energy, (2) the neutral-interstitial-formation energy, and (3) the various ionization levels for charged species.

We visualize the formation of a neutral vacancy in the solid in several steps as listed in Table II, together with the changes in thermodynamic potential or Gibbs free energy that accompany each hypothetical step. This table shows the steps involved in creating a cation vacancy in $\text{Hg}_{1-x}\text{Cd}_x\text{Te}$ by removing one cation to the surface and leaving a vacant site behind. A similar development may be made for anion vacancies. In Table II there are N Hg atoms in the crystal, $N/(1-x)$ cations including both Cd and Hg, and a total number of bonds, $N_b \approx 4N(1-x)$. There are N_v neutral cation vacancies already in the crystal. (Here and in what follows we assume that the concentrations of all native defects $\ll 1$.) The total change in Gibbs free energy is obtained by adding up the contributions from each step. P_{ext} is the external pressure and ΔV_s is the volume change of the crystal upon the addition of one more cation site. The crucial assumption used in Table II is the macroscopic cavity model,^{3,4} which states that when a vacancy is formed in a metal with the same average electron density as the semiconductor, the surface energy around the "cavity" of the vacancy is given by the surface tension of a free-electron gas, and the surface area of the cavity is that of an octahedron with all (111) surfaces, containing one atomic volume. For a vacancy formed in a semiconducting crystal, the extra energy required to break the covalent bonds between the removed atom and its neighbors must be added.

A solid not in contact with an external phase is theoretically convenient but experimentally irrelevant, so we must consider equilibrium with liquid or vapor. When

the solid is in contact with a liquid or gas into which atoms can escape, the equilibrium condition is given by the free-energy change for creation of a vacancy by escape of an atom into the gas or liquid. Several additional terms enter this free energy. Table III lists the steps involved in taking a Hg atom from a sample of $\text{Hg}_{1-x}\text{Cd}_x\text{Te}$ containing N Hg atoms into the liquid or gas, leaving behind a vacant cation site. The gas is assumed to be ideal, i.e., effects of association are taken into account for the liquid only. Temperature variation of $P_{0,\text{Hg}}$, L_V , and ΔS_F is neglected, so these parameters can be easily obtained by fitting experimental vapor pressures for the pure elements in the desired temperature range, or directly from tables of experimental results.

For a crystal in equilibrium with the liquid or gas phase, the calculations should yield the same cation-vacancy concentration, independent of whether we visualize a mercury or cadmium atom leaving the crystal. Table III shows the changes in free energy for removing one Hg atom from the crystal. If we want to remove one Cd, T_F , ΔS_F , L_V , ΔV , $P_{0,\text{Hg}}$, P_{Hg} , a_{Hg}^* , and C_{Hg} will be replaced by the appropriate quantities for Cd. $N/(1-x)$ will be replaced by N/x wherever it appears, for N now refers to the total number of Cd atoms in the crystal, so that the total number of cations is N/x . Also, the first factor in front of the E'_b term in step 4 will be $-(1-x)$ instead of x . The principal difference between equilibrium of the solid with no accessible external phase and equilibrium with a liquid (or vapor) is that the composition of the crystal is altered by the departure of a Hg or Cd atom. Since the bond energy of CdTe is higher than that of HgTe, it becomes more favorable in the mixed compound for Hg to leave, and this is reflected in the $[\text{Hg}]/[\text{Cd}]$ concentration ratio in the fluid.

These expressions for the change in free energy required

TABLE III. Steps in cation-vacancy formation (equilibrium with Hg in liquid or gas phase). T_F and ΔS_F denote temperature and entropy of fusion for pure Hg; c_{Hg} and a_{Hg}^* denote concentration and activity coefficient for Hg in the melt; P_{Hg} and $P_{0,\text{Hg}}$ denote Hg partial pressure in solid-vapor equilibrium and Hg vapor pressure extrapolated to infinite temperature; L_V denotes latent heat of vaporization (pure Hg); P_{ext} denotes external pressure; ΔV denotes volume of one Hg atom in the melt; E'_b denotes dE_b/dx .

Step	Change in Gibbs free energy (ΔG)
	$\Delta G_L(\text{Hg}) = \Delta G_1 + \Delta G_{2a} + \Delta G_3 + \Delta G_4 + \Delta G_5$ $\Delta G_G(\text{Hg}) = \Delta G_1 + \Delta G_{2b} + \Delta G_3 + \Delta G_4 + \Delta G_5$
(1) crystal(N) \rightarrow metal(N)	$N_b E_b$
(2a) metal(N) \rightarrow metal($N-1$) + Hg(in liquid)	$\Delta S_F(T_F - T) + P_{\text{ext}} \Delta V - P_{\text{ext}} \Delta V_S$ $- k_B T \ln(1-x) + k_B T \ln(c_{\text{Hg}} a_{\text{Hg}}^*)$
or	
(2b) metal(N) \rightarrow metal($N-1$) + Hg(in gas)	$\Delta S_F(T_F - T) + P_{\text{ext}} \Delta V - k_B T \ln(1-x) - P_{\text{ext}} \Delta V_S$ $+ L_V - k_B T \ln(P_{0,\text{Hg}})$ $+ k_B T \ln(P_{\text{Hg}})$
(3) metal($N-1$) \rightarrow metal($N-1$) + cavity	$\Delta H_m + k_B T \ln[N_v(1-x)/N] + P_{\text{ext}} \Delta V_S$
(4) metal($N-1$) + cavity \rightarrow crystal($N-1$) + cavity	$-(N_b - 4)[E_b + x(1-x)(E'_b/N)]$
(5) Jahn-Teller distortion of cavity	$-k_B T \ln 3$

to create a cation vacancy by removing either a Cd or Hg atom were derived by assuming that the placement of Cd and Hg in the crystal is essentially random, so the environment of the cavity left behind is not correlated with the cation species which occupied the site. If like cations have a tendency to cluster or anticluster, then a more complicated analysis must be done, calculating the expected densities of vacancies in different environments separately. We have compared cation vacancy densities calculated from these simple expressions, assuming equilibrium with both the gas and the liquid melt at the maximum melting point for CdTe, and focusing on both the Cd and Hg equilibrium for $\text{Hg}_{0.8}\text{Cd}_{0.2}\text{Te}$ growth at 825 K from a Te-rich solution. Calculating the defect densities expected under certain conditions from two different sets of equilibrium relations, both of which should be satisfied, should give identical results, if all the approximations made are exact. We comment in a following section on the results of these valuable checks.

It seems worthwhile to point out that in the absence of the environmental effects or clustering just mentioned, it is meaningless to distinguish Hg vacancies from Cd vacancies. This very elementary fact seems to have been misunderstood in some of the literature and is quite independent of the tendency of Hg to leave the mixed compound under most external conditions.

When an interstitial is formed, a rather different set of considerations enters. Van Vechten² gives a prescription for calculating the enthalpy of formation of simple interstitials. This prescription gives enthalpies of formation equal to $Z E_g / 2$, where Z is the effective valence of the interstitial. As noted earlier, these enthalpies of formation are very large, and would result in negligible concentrations of interstitials, particularly for anion interstitials, which have $Z = 6$. Therefore, any appreciable neutral interstitial concentrations must be due to semibonded interstitials and not to simple interstitials. In the absence of a theoretical determination of the enthalpy of formation for neutral self-interstitials, I_0 , we have used values in the range 1–2 eV, which are somewhat lower than estimates of enthalpies of formation for self-interstitials in copper calculated by Huntington and Seitz,^{8,9} due to the less-close-packed structure. Differences in relaxation of the lattice around cation and anion interstitials should lead to somewhat different enthalpies of formation for these; however, we use the same I_0 for both cation and anion interstitials. There is clearly much room for improvement in providing better estimates of interstitial formation enthalpies.

There is also a fundamental reason for disagreeing with Van Vechten's prescription for the creation energy for simple interstitials: it is justified as the energy required to take Z electrons from the Fermi level to localized states, composed of conduction-band states, around the interstitial core. However, the removal of the interstitial from a bonding site at the surface or from the external phase involves the removal of the Z electrons associated with it from orbitals far down in the valence band, or in low-energy atomic like states, as well as states near the Fermi level. These electrons, which were surrounding the interstitial core in the external phase or in a bonding site in the

crystal, are removed to the localized interstitial levels, or to the Fermi level, while other free electrons come from the Fermi level to neutralize the interstitial core. The part of the neutral-interstitial-formation energy resulting from the removed electronic states is therefore not correctly accounted for in Van Vechten's picture.

Adding up all the contributions to the free energy for an atom leaving the surface to become an interstitial, and assuming as we did for vacancies that the defect concentrations $\ll 1$, and also that $N_b \approx 4$ times the total number of cations, we have, for the Gibbs free energy of breaking two bonds and moving one Hg atom from a lattice site at the surface to become a neutral Hg interstitial,

$$\begin{aligned} \Delta G_I(\text{Hg}) &= 2E_b + I_0 + k_B T \ln(N_{\text{Hg}}/N_C) \\ &\quad - P_{\text{ext}} \Delta V_S - k_B T \ln(1-x) - 4xE'_b \\ &= \Delta H(I_{\text{Hg}}^x) + k_B T \ln \left[\frac{N_{\text{Hg}}}{N_C(1-x)} \right], \end{aligned} \quad (1)$$

where N_{Hg} is the total number of neutral Hg interstitials and N_C is the number of cation interstitial sites, which is equal to the total number of cation sites on the lattice. [The cation interstitial sites are assumed to be the sites of the alternate cation sublattice, displaced from the Te sublattice by $(-0.25, -0.25, -0.25)a$, if the cation sublattice is displaced by $(0.25, 0.25, 0.25)a$.] The changes in free energy for a Hg atom leaving the liquid or gas phase to become a neutral interstitial will have an additional contribution of

$$\begin{aligned} \Delta S_F(T - T_F) - P_{\text{ext}} \Delta V - k_B T \ln(c_{\text{Hg}} a_{\text{Hg}}^*) \\ - 2E_b + 4xE'_b + k_B T \ln(1-x) + P_{\text{ext}} \Delta V_S \end{aligned}$$

for the liquid, and

$$\begin{aligned} \Delta S_F(T - T_F) - P_{\text{ext}} \Delta V - k_B T \ln(P_{\text{Hg}}) \\ - L_V + k_B T \ln(P_{0,\text{Hg}}) \\ - 2E_b + 4xE'_b + k_B T \ln(1-x) + P_{\text{ext}} \Delta V_S \end{aligned}$$

for the gas. ΔV_S is the volume in the solid occupied by one cation site and ΔV is the volume of one Hg atom in the liquid. The changes in free energy for creation of neutral Cd interstitials are obtained by replacing $\ln(1-x)$ by $\ln x$ and $-4xE'_b$ by $4(1-x)E'_b$, and using c_{Cd} , P_{Cd} , and other quantities appropriate for Cd. The changes in free energy for creation of neutral Te interstitials are obtained by removing the E'_b term and using quantities appropriate for Te.

The above approximations for the free energies of formation of vacancies and interstitials become invalid when the defect concentrations are so large that interactions among them become important. We have assumed that the defects behave as ideal gases, with chemical potentials proportional to their concentrations.

Since charged native defects dominate strongly over neutral native point defects in these ionic materials, it is not sufficient to calculate enthalpies of formation of neutral native defects. The ionization levels also play an important role in determining total defect concentrations. Calculation of the ionization levels is complicated by the

TABLE IV. Parameters for defects in $\text{Hg}_{1-x}\text{Cd}_x\text{Te}$.

Symbol	Description	Defining relations
a	Lattice constant	$a(300\text{ K}) + a'(300\text{ K})(T - 300\text{ K})$
m_e^*	electron effective mass ($m_0 = \text{free-}e^- \text{ mass}$)	CdTe: $m_e^*(T) = 0.096E_0(0)/E_0(T)$ $\text{Hg}_{0.8}\text{Cd}_{0.2}\text{Te}$: $m_e^*(T) = f(E_0(T))$
m_h^*	Hole effective mass	CdTe: $m_h^* = 0.63E_0(0)/E_0(T)$ $\text{Hg}_{0.8}\text{Cd}_{0.2}\text{Te}$: $m_h^* = g(E_0(T))$
E_0	Fundamental gap	$E_0(T) = E_0(300\text{ K}) + E'_0(300\text{ K})(T - 300\text{ K})$
E_1^C	First ionization level of cation vacancy	$E_1^C(T) = E_1^C(0) + 0.7826f_1TE_0(300\text{ K})$
E_2^C	Second ionization level of cation vacancy	$E_2^C(T) = E_2^C(0) + 0.7826f_1TE_0(300\text{ K})$
E_1^A	First ionization level of anion vacancy	$E_1^A(T) = E_1^A(0) + (1 - 0.2174f_1)TE'_0(300\text{ K})$
E_2^A	Second ionization level of anion vacancy	$E_2^A(T) = E_2^A(0) + (1 - 0.2174f_1)TE'_0(300\text{ K})$
I_1^C	First ionization level of cation interstitial	$I_1^C(T) = I_1^C(0) + (1 - 0.2174f_1)TE'_0(300\text{ K})$
I_2^C	Second ionization level of cation interstitial	$I_2^C(T) = I_2^C(0) + (1 - 0.2174f_1)TE'_0(300\text{ K})$
I_1^A	First ionization level	$I_1^A(T) = I_1^A(0) + 0.7826f_1TE'_0(300\text{ K})$
I_2^A	Second ionization level of anion interstitial	$I_2^A(T) = I_2^A(0) + 0.7826f_1TE'_0(300\text{ K})$
f_i	Fraction of localized character in ionization levels	
E_F	Self-consistent Fermi energy (solid equilibrium)	
$\Delta H(V_C^{\bar{c}})$	Enthalpy of formation of neutral cation vacancy	$\Delta H_{m,c} + 2E_b$ ($P_{\text{ext}}\Delta V \approx 0$)
I_0	Enthalpy of formation of neutral interstitial	
C'	Concentration derivative of ionic gap, i.e., dC/dx	Table I
E'_h	dE_h/dx	
E'_g	dE_g/dx	
D'	dD/dx	
E'_b	dE_b/dx	
$F_{1/2}(\gamma)$	Fermi-Dirac function	$e^\gamma/(1 + ae^\gamma)$ $\tilde{a} = 0.0$ for $\gamma = 1.5$ $\tilde{a} = 0.25$ for $-1.5 < \gamma < 2.5$

TABLE IV. (Continued).

Symbol	Reference	Value at 300 K for CdTe	Value at ^a 1365 K for CdTe	Value at 300 K for Hg _{0.8} Cd _{0.2} Te	Value at ^a 825 K for Hg _{0.8} Cd _{0.2} Te
a	29, 30 (CdTe) 34, 35 (Hg _{0.8} Cd _{0.2} Te)	6.482 Å	6.523 Å	6.466 Å	6.486 Å
m_e^*	31 (CdTe) 32, Fig. 37 (Hg _{0.8} Cd _{0.2} Te)	0.102 m_0	0.134 m_0	0.012 m_0	0.021 m_0
m_h^*	33 (CdTe) 32, Eq. (26) (Hg _{0.8} Cd _{0.2} Te)	0.672 m_0	0.877 m_0	0.467 m_0	0.467 m_0
E_0	21, 36 (CdTe) 17, 22 (Hg _{0.8} Cd _{0.2} Te)	1.501 eV	1.150 eV	0.1623 eV	0.2935 eV
E_1^C	2, 27	0.05 eV	-0.1700 eV	-0.4580 eV	-0.3759 eV
E_2^C	2, 27	0.85 eV	0.6300 eV	0.0490 eV	0.1311 eV
E_1^A	2, 27	1.491 eV	1.201 eV	0.1393 eV	0.2477 eV
E_2^A	2, 27	1.466 eV	1.176 eV	0.1193 eV	0.2277 eV
I_1^C	2, 27	1.491 eV	1.201 eV	0.1429 eV	0.2741 eV
I_2^C	2, 27	1.326 eV	1.036 eV	0.0841 eV	0.2153 eV
I_1^A	2, 27	0.15 eV	-0.0700 eV	0.0570 eV	0.1391 eV
I_2^A	2, 29	0.9 eV	0.6800 eV	0.0670 eV	0.1491 eV
f_l		0.8	0.8	0.8, 0.0 for I_C	0.8, 0.0 for I_C
E_F		0.8317 eV	0.6962 eV	0.1541 eV	0.2588 eV
$\Delta H(V_C^*)$	Table II	2.350 eV 1.65 eV	2.317 eV 1.65 eV	1.534 eV 1.65 eV	1.540 eV 1.65 eV
I_0				0.1428 eV	0.1421 eV
E_h'	Table I			0.1551 eV	0.1539 eV
E_g'	Table I			0.2067 eV	0.2054 eV
D'	Table I			0.5074 eV	0.4671 eV
E_b'	Table I			0.1329 eV	0.1223 eV

^aThese are typical temperatures of growth in liquid-phase methods.

fact that vacancy levels are generally associated with electrons bound in quite localized orbits,¹ so that the effective-mass approximation cannot be used. The two bound electrons of I_{Te}^{-2} should also be quite localized, or else these interstitials would not have a sufficiently high mobility to contribute as strongly to Te self-diffusion as seems to be the case. Experimentally identified cadmium interstitial ionization levels at 300 K in CdTe also do not correspond very well to levels calculated from effective-

mass theory. For CdTe we have chosen to use the *identified*²⁷ ionization levels for all native defects, and to treat all charged states as if they involve quite localized bound carriers. There does not seem to be such a complete set of identified native-defect ionization levels in Hg_{0.8}Cd_{0.2}Te as for CdTe, so we have been forced to choose plausible low-temperature levels. For Hg_{0.8}Cd_{0.2}Te, we use the cation interstitial levels predicted by effective-mass theory, assuming that the cation interstitial bound states are hy-

drogenic orbits spread out over many unit cells, while the other native-defect bound states in $\text{Hg}_{0.8}\text{Cd}_{0.2}\text{Te}$, as for CdTe, are well localized. We take the second cation-vacancy ionization level at ~ 2 meV for $T=0$ K, consistent with the determination by Jones.²⁸ We let the first ionization level be 0.507 eV below the second ionization level in $\text{Hg}_{0.8}\text{Cd}_{0.2}\text{Te}$, which corresponds to a level well below the band edge. These are not the positions commonly attributed to these levels. In particular, our assignments disagree with assignment of the tunneling centers to the second vacancy level. Further experimental work identifying low-temperature bare native-defect ionization levels in Hg-rich $\text{Hg}_{1-x}\text{Cd}_x\text{Te}$ would be very useful to us in determining ionization levels and equilibrium defect densities at high temperature. In order to allow for the temperature dependence of these ionization levels, we first divide the temperature dependence of the fundamental gap, E_0 , into a part due to the free hole (78.3%) and a part due to the free electron (21.7%).⁶ Following Van Vechten,¹ we then let the temperature dependence of an acceptor level measured from the valence band be equal to $f_1(0.783dE_0/dT)$, where f_1 is the fraction of localized character in the acceptor level, or conversely, $1-f_1=f_e$ is the fraction of extended character. We let the temperature dependence of a donor level measured from the conduction band be $f_1(0.217dE_0/dT)$. For CdTe and $\text{Hg}_{0.8}\text{Cd}_{0.2}\text{Te}$ we choose $f_1=0.8$, except for cation interstitials in $\text{Hg}_{0.8}\text{Cd}_{0.2}\text{Te}$, where we use $f_1=0$.

To summarize, Tables IV and V collect together the quantities used in computing equilibrium densities of defects and intrinsic carriers. The effective masses m_e^* and m_h^* were scaled following Weiler³² for $\text{Hg}_{0.8}\text{Cd}_{0.2}\text{Te}$, and for CdTe the low-temperature values were scaled as a function of E_0 by assuming that gaps for all states near the fundamental gap decrease proportionally with T , as would be expected if neighboring gaps decreased with the same Debye-Waller factor.

The electron and hole densities are computed using the approximation given in Table IV for the Fermi-Dirac integral $F_{1/2}(\gamma)$. The parameter $\bar{a}=0.0$ for nondegenerate

statistics, i.e., $\gamma < -1.5$ (all cases considered for CdTe), and $\bar{a}=0.25$ for moderately degenerate statistics, i.e., $\gamma < 2.5$ ($\text{Hg}_{0.8}\text{Cd}_{0.2}\text{Te}$). We do not consider cases where $\gamma > 2.5$. This approximate form is correct to within about 5% for the listed range of γ .

The values listed for L_V and p_0 in Table V are fitted to vapor-pressure data³⁷ from 700 to 1200 K for Cd and Te, and from 300 to 900 K for Hg; therefore, L_V is not necessarily equal to the latent heat of vaporization at the normal boiling temperature for these elements. The quantities for Te refer to the vapor pressure of monatomic Te gas, which is in equilibrium with a larger vapor pressure of Te_2 gas at each temperature.

D. Mass-action equations and charge balance

Finally, we turn to the equilibrium thermodynamics (or mass-action equations) needed for the computation of the defect densities. Using the equilibrium condition that the change in Gibbs free energy to create one more defect is zero, we obtain the mass-action equations summarized in Table VI. These equations were derived using the relations for the solid in equilibrium with no accessible external phase. There are analogous equations for equilibrium with the gas or liquid. The total concentration of cation interstitials is given by the sum of the Hg and Cd interstitial concentrations, $[I_C]=[I_{\text{Hg}}]+[I_{\text{Cd}}]$. The ionization levels are assumed to be the same for Cd and Hg interstitials. The free-energy changes for creation of anion vacancies and interstitials are calculated in the same way as for cation vacancies and interstitials. The Jahn-Teller distortion is assumed to exist for neutral and singly ionized vacancies (which have a filled- or empty-shell configuration). This gives rise to a factor of $\frac{1}{3}$ in the equations for the doubly ionized vacancies. The extra factors of 2 and $\frac{1}{2}$ in the equations for ionized defects are due to spin degeneracy.

Now we have assembled all the material needed to calculate the defect concentrations. The final equation is the charge-balance equation:

TABLE V. Atomic parameters for defects in $\text{Hg}_{1-x}\text{Cd}_x\text{Te}$.

Symbol	Description	Reference	Hg	Cd	Te
T_F	Temperature of fusion (K)	37	234.0	594.18	722.65
ΔS_F	Entropy of fusion (eV/K atom)	37	1.026×10^{-4}	1.080×10^{-4}	2.506×10^{-4}
L_V	Latent heat of vaporization (eV/atom)	37	0.606	1.030	1.798
P_0	Extrapolated infinite T vapor pressure (atm)	37	7.36×10^4	1.004×10^5	1.486×10^5
a^*	Activity in liquid $\text{Hg}_{0.2}\text{Cd}_{0.02}\text{Te}_{0.78}$, 825 K	38	0.127	4.3×10^{-5}	1.0
	$\text{Cd}_{0.5}\text{Te}_{0.5}$, 1365 K	39		0.3	0.27

$$[h^+] + [I_C^+] + [V_A^+] + 2[I_C^{+2}] + 2[V_A^{+2}] - 2[I_A^{-2}] - 2[V_C^{-2}] - [I_A^-] - [V_C^-] - [e^-] = 0. \quad (2)$$

From Table VI we express each term in the above equation in terms of the Fermi energy. There results a polynomial equation for $y \equiv \exp[E_F/(k_B T)]$:

$$\begin{aligned} & \left[\frac{2\bar{a}b}{3} \right] \{ [V_C^X] \exp[-(E_1^C + E_2^C)/(k_B T)] + 3[I_A^X] \exp[-(I_1^A + I_2^A)/(k_B T)] \} y^6 \\ & + \left[2\bar{a}b \{ [V_C^X] \exp[-E_1^C/(k_B T)] + [I_A^X] \exp[-I_1^A/(k_B T)] \} \right. \\ & + \left. \left[\frac{2b'}{3} \right] \{ [V_C^X] \exp[-(E_1^C + E_2^C)/(k_B T)] + 3[I_A^X] \exp[-(I_1^A + I_2^A)/(k_B T)] \} \right] y^5 \\ & + \left[\left[\frac{2\bar{a}}{3} \right] \{ [V_C^X] \exp[-(E_1^C + E_2^C)/(k_B T)] + 3[I_A^X] \exp[-(I_1^A + I_2^A)/(k_B T)] \} \right. \\ & + \left. 2b' \{ [V_C^X] \exp[-E_1^C/(k_B T)] + [I_A^X] \exp[-I_1^A/(k_B T)] \} + 2b \left[\frac{m_e^* k_B T}{2\pi\hbar^2} \right]^{3/2} \right] y^4 \\ & + \left[2\bar{a} \{ [V_C^X] \exp[-E_1^C/(k_B T)] + [I_A^X] \exp[-I_1^A/(k_B T)] \} \right. \\ & - \left. 2\bar{a}b \left[[I_C^X] \exp[I_1^C/(k_B T)] + [V_A^X] \exp[E_1^A/(k_B T)] + \left[\frac{m_h^* k_B T}{2\pi\hbar^2} \right]^{3/2} \right] + 2\bar{a}b \left[\frac{m_e^* k_B T}{2\pi\hbar^2} \right]^{3/2} \right] y^3 \\ & - \left[\left[\frac{2\bar{a}b}{3} \right] \{ 3[I_C^X] \exp[(I_1^C + I_2^C)/(k_B T)] + [V_A^X] \exp[(E_1^A + E_2^A)/(k_B T)] \} \right. \\ & + \left. 2b' \{ [I_C^X] \exp[I_1^C/(k_B T)] + [V_A^X] \exp[E_1^A/(k_B T)] \} + 2 \left[\frac{m_h^* k_B T}{2\pi\hbar^2} \right]^{3/2} \right] y^2 \\ & - \left[2\bar{a} \{ 3[I_C^X] \exp[I_1^C/(k_B T)] + [V_A^X] \exp[E_1^A/(k_B T)] \} \right. \\ & + \left. \left[\frac{2b'}{3} \right] \{ 3[I_C^X] \exp[(I_1^C + I_2^C)/(k_B T)] + [V_A^X] \exp[(E_1^A + E_2^A)/(k_B T)] \} \right] y \\ & - \left[\frac{2\bar{a}}{3} \right] \{ 3[I_C^X] \exp[(I_1^C + I_2^C)/(k_B T)] + [V_A^X] \exp[(E_1^A + E_2^A)/(k_B T)] \} = 0, \quad (3a) \end{aligned}$$

where

$$b = e^{-E_0/(k_B T)} \quad (3b)$$

and

$$b' = 1 + 2\bar{a}b. \quad (3c)$$

This polynomial equation is easily solved numerically and expressions for the different defect densities are obtained.

In the case of samples quenched rapidly from annealing temperatures of ~ 600 – 700 to 77 K, so that the net deviation from stoichiometry is frozen in as majority point defects, which do not have time to combine into complexes and extended defects, we assume that only electronic equilibrium is reached at 77 K. Charge-carrier densities and charged defect densities are then calculated at 77 K by use of Eq. (2), as before, except that the total number of majority defects is frozen-in, and an initial starting value of E_F , $E_F^{(0)}$, is used to determine the proportion of these defects which are neutral, instead of using the equilibrium concentrations of neutral defects. After the equation is solved, the resulting value of E_F is used as the

next starting value, and this procedure is iterated until a self-consistent solution is reached.

We conclude this section by emphasizing that we are computing the mass-action constants wherever possible, and not fitting them to experiment. This is particularly valuable to (1) turn off the production of one or other defect species artificially, in order to examine the important reactions in equilibrium, (2) to examine new materials that might be proposed to improve the structural quality of the starting semiconductor, and (3) to reveal inconsistencies between the present understanding of formation enthalpies of defects, proposed identifications of native-defect ionization levels, and experimental work on defect and charge-carrier concentrations.

As is well known, the strength and electrical properties of a semiconductor may be largely due to macroscopic defects (dislocations, including voids). Formation of extended defects and the concentrations of point defects remaining at lower temperatures are not determined solely by equilibrium concentrations of native defects during growth and annealing. They also depend strongly on ki-

TABLE VI. Mass-action equations. The square brackets are used for concentration. Different charge states are shown by superscripts, and the superscript X is used for neutral defects. N_S is the number of atom pairs per unit volume. m_h^* and m_e^* are the effective masses of (heavy) holes and electrons. The small contribution of the light holes is neglected. Cation interstitials and vacancies in the cation sublattice are denoted by I_C and V_C , and anion vacancies and interstitials are denoted by V_A and I_A .

$[V_C^X] = 3N_S e^{-\Delta H(V_C^X)/(k_B T)}$	$[V_A^+] = 2[V_A^X] e^{(-E_F + E_1^A)/(k_B T)}$
$[V_A^X] = 3N_S e^{-\Delta H(V_A^X)/(k_B T)}$	$[V_A^{+2}] = \frac{1}{6}[V_A^+] e^{(-E_F + E_2^A)/(k_B T)}$
$[I_A^X] = N_S e^{-\Delta H(I_A^X)/(k_B T)}$	$[I_A^-] = 2[I_A^X] e^{(E_F - I_1^A)/(k_B T)}$
$[I_Cd^X] = xN_S e^{-\Delta H(I_Cd^X)/(k_B T)}$	$[I_A^{-2}] = \frac{1}{2}[I_A^+] e^{(E_F - I_2^A)/(k_B T)}$
$[I_{Hg}^X] = (1-x)N_S e^{-\Delta H(I_{Hg}^X)/(k_B T)}$	$[I_C^+] = 2[I_C^X] e^{(-E_F + I_1^C)/(k_B T)}$
$[I_C^X] = [I_Cd^X] + [I_{Hg}^X]$	$[I_C^{+2}] = \frac{1}{2}[I_C^X] e^{(-E_F + I_2^C)/(k_B T)}$
$[V_C^-] = 2[V_C^X] e^{(E_F - E_1^C)/(k_B T)}$	$[h^+] = 2 \left[\frac{m_h^* k_B T}{2\pi h^2} \right]^{3/2} F_{1/2}\{-E_F/(k_B T)\}$
$[V_C^{-2}] = \frac{1}{6}[V_C^-] e^{(E_F - E_2^C)/(k_B T)}$	$[e^-] = 2 \left[\frac{m_e^* k_B T}{2\pi h^2} \right]^{3/2} F_{1/2}\{(E_F - E_C)/(k_B T)\}$

netic barriers to point-defect migration, and on interactions between point defects, including the formation of complexes of native defects with other native defects or impurities. We will discuss these questions in a subsequent paper. In the next two sections we will present some results on equilibrium concentrations of native point defects expected at various temperatures for CdTe and $\text{Hg}_{0.8}\text{Cd}_{0.2}\text{Te}$. These results mark out the approximate bounds on the structural quality that microscopic atomic mechanisms offer to the semiconductor maker.

III. RESULTS FOR CdTe

Let us begin by comparing the results of this analysis to Hall experiments done at high temperature,²⁷ where equilibrium densities of simple point defects should determine the electrical behavior. Since the external pressure of Cd was controlled in these experiments, we must find the Te pressure which would be in equilibrium at each T and P_{Cd} . From a fit to equilibrium Te and Te_2 vapor pressures,³⁷ we obtain

$$P_{\text{Te}} = (472 \text{ atm}^{1/2})(P_{\text{Te}_2})^{1/2} \exp[-(1.174 \text{ eV})/(k_B T)].$$

The change in free energy for congruent sublimation of one atom pair from CdTe is

$$\begin{aligned} \Delta G_{\text{CS}} = & 4E_b + L_{v,\text{Cd}} + \Delta S_{F,\text{Cd}}(T_{F,\text{Cd}} - T) \\ & + L_{v,\text{Te}} + \Delta S_{F,\text{Te}}(T_{F,\text{Te}} - T) \\ & + \ln(P_{\text{Cd}}/P_{0,\text{Cd}}) + \ln(P_{\text{Te}}/P_{0,\text{Te}}). \end{aligned}$$

Using the condition that $\Delta G_{\text{CS}} = 0$ for P_{Cd} and P_{Te} in equilibrium, expressing P_{Te} in terms of P_{Te_2} , and using

values appropriate for 950–1100 K, we obtain

$$\begin{aligned} (P_{\text{Te}_2})^{1/2} = & (2.04 \times 10^9 \text{ atm}^{3/2}) \\ & \times \exp[-(2.753 \text{ eV})/(k_B T)]/P_{\text{Cd}}. \end{aligned}$$

This calculated expression compares favorably with the expression derived from a fit to experiments from 1053 to 1212 K (Eq. 1.6 of Ref. 40):

$$\begin{aligned} (P_{\text{Te}_2})^{1/2} = & (6.61 \times 10^9 \text{ atm}^{3/2}) \\ & \times \exp[-(2.97 \text{ eV})/(k_B T)]/P_{\text{Cd}}. \end{aligned}$$

Figure 1 shows the electron concentrations obtained from this analysis, compared to those obtained from Hall experiments²⁹ for different P_{Cd} at 1088 and 963 K. This fit was obtained using $I_0 = 1.65 \text{ eV}$ and $f_1 = 0.8$ for all the charged defect levels. Since the identified cation interstitial levels at 300 K ($E_0 = 0.01$ and 0.175 eV) are not equal to those predicted by the effective-mass approximation ($E_0 = 0.014$ and 0.058 eV), if the identifications are correct, they must correspond to electron bound states closer to the interstitial atom than a hydrogenic model would give. Small adjustments in the localized character of the bound states for ionized defects, $f_1 \approx 0.8$, and in the enthalpy of formation of a neutral interstitial, I_0 , including use of a different I_0 for cation and anion interstitials, will affect the calculated electron densities. However, the approximations we have made do give a reasonable fit to the measured electron densities, using the proposed 300-K ionization levels for charged defects and the calculated temperature dependences and enthalpies of formation for neutral vacancies.

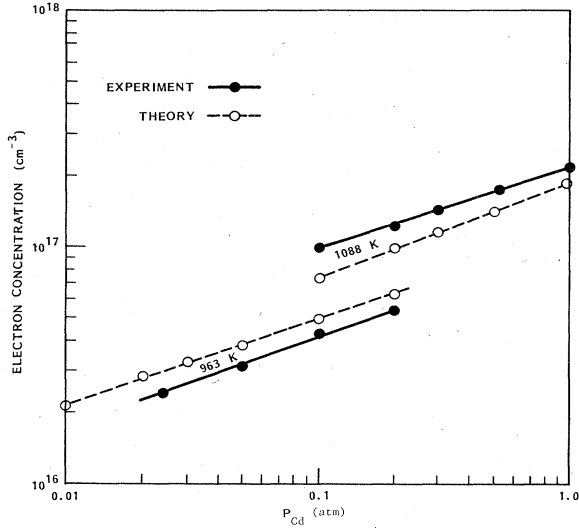


FIG. 1. CdTe solid in equilibrium with vapor. The experimental curves are the results of Hall measurements from Ref. 27 (see text).

An advantage of calculating the enthalpies of defect formation and the temperature dependences of ionization levels, wherever possible, is that it then becomes possible to identify separately densities of many different donor and acceptor defects without relying on fits using a large number of parameters. It is also possible to artificially "turn off" production of particular defects at will, in order to see the effect on equilibrium concentrations of other impurities. Figure 2 shows the concentrations of all the charged native defects contributing to the total excess electron concentration at 1088 K. The open symbols show the equilibrium densities of the donors which would be seen if the acceptors were suppressed. Since CdTe is a wide-gap semiconductor, the Fermi level is not fixed by the intrinsic carriers, but can be affected by the charged donor and acceptor densities. Increasing concentrations of charged acceptors lower E_F , making it easier to create more charged native donor defects. As P_{Cd} is increased, the donor defects become more dominant, so the effect of compensation in increasing charged native-donor-defect concentrations is reduced.

Although in the usual experimental situations of growth and annealing, the alloy is in contact with an external phase to which the atoms can escape, and thus the equilibrium densities of native defects in the alloy are strongly influenced by external conditions such as the concentration and activity of each element in the liquid, or the partial pressures of each element in the gas phase, it is instructive to study the native-defect densities expected for the solid in equilibrium when it is not in contact with an external phase to which atoms can escape. In this way we can separate out effects due to varying conditions in the external phase, and focus on effects due to the basic nature of the material. Figure 3 shows the densities for all the charged native defects in equilibrium in the absence of an accessible external phase, together with the majority charged-defect densities which would be seen in

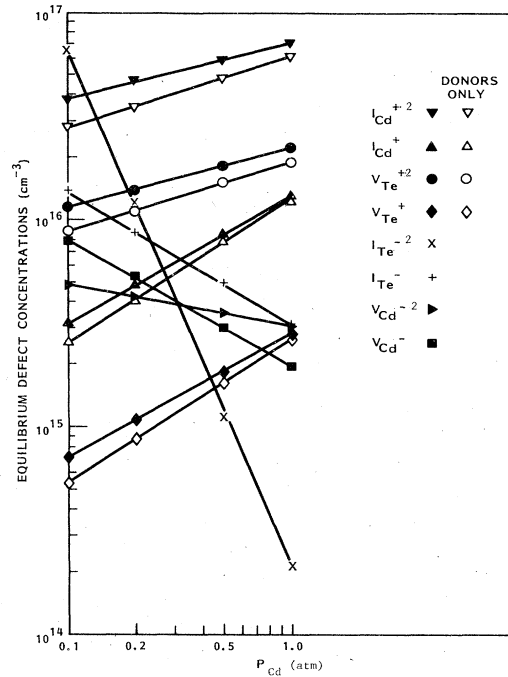


FIG. 2. Theoretical equilibrium defect concentrations at 1088 K for CdTe solid-vapor equilibrium.

the absence of the minority charged defects, over a wide range of temperature. The usual exponential temperature dependence which holds at lower temperature is modified as the temperature approaches the maximum melting point, 1365 K, and the increasing charged-defect densities affect the Fermi level and begin to saturate. Compensa-

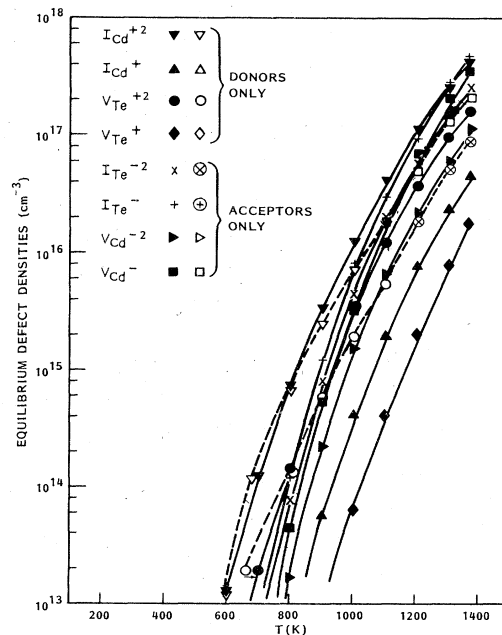


FIG. 3. CdTe solid with no external phase. These theoretical results are illustrative of intrinsic properties and have no direct experimental significance.

tion becomes increasingly important at higher temperatures: the majority defect densities are strongly increased by the presence of minority charged defects. In fact, the alloy changes from p type at 1365 K to n type around 900 K and below, as the balance between the closely competing charged native donor and acceptor defects shifts. Neutral defect densities are several orders of magnitude lower than charged-defect densities in all cases: favorable ionization levels are a major cause of high defect concentrations in CdTe.

Small changes in such quantities as the fraction of localized character in the bound states of the charged defects, f_1 , can alter the relative positions of charged-defect species with nearly equal concentrations. However, the basic result that CdTe is a highly compensated material with high charged-defect concentrations at high temperature, due to favorable ionization energies and the large gap, which suppresses intrinsic carrier formation, is expected to be insensitive to small modifications. This basic result may help to explain the widespread difficulties with impurity contamination and with dislocation formation in CdTe grown near 1365 K, as large concentrations of native defects (several times the net deviation from stoichiometry) may serve as nucleation centers for extended defects and impurities.

Precise prediction of experimental results requires complete consideration of the external phase in contact with the alloy when it is brought into equilibrium, as well as consideration of the alloy isolated from contact with an external phase. We have used experimentally determined activities and rough fits for the vapor pressures, as we are not interested in developing a theory for the liquid or gas phase. In order to check the accuracy of this description of the gas and the liquid in equilibrium with the alloy, we list in Table VII the total vacancy and interstitial concentrations for both cations and anions expected for CdTe in equilibrium at 1365 K. At this temperature, the solid is in equilibrium with the gas for $P_{\text{Cd}}=0.65$ atm and $P_{\text{Te}_2}=0.0055$ atm,⁴⁰ and with the liquid for $c_{\text{Cd}}=0.5$ and $c_{\text{Te}}=0.5$. Equilibrium native-defect densities should be the same for equilibrium with the liquid and the gas at these concentrations and pressures, if we have correctly understood these phases. Table VII therefore gives a rough measure of the error in our estimated defect densities resulting from the crudeness of our approximations. The defect densities for the solid in equilibrium with no external phase available fit nearly between the values for the liquid and gas equilibria, showing that both the liquid and the gas results are in error in different directions. Summing up, we obtain $(4.2-5.1)\times 10^{17}/\text{cm}^3$ excess Te

in equilibrium at 1365 K, in comparison to the experimental value⁴⁰ of $\sim 1.5\times 10^{17}/\text{cm}^3$. Since this net deviation from stoichiometry results from the difference of several comparable terms with considerable uncertainty in each term, we consider this quite acceptable agreement. It is also likely that, for these high defect concentrations, the formation and ionization energies of the defects are modified by overlap effects, which we have neglected.

Original suggestions for improving the crystal quality of CdTe/ $\text{Hg}_{0.8}\text{Cd}_{0.2}\text{Te}$ epilayer junctions by using $\text{Cd}_{0.96}\text{Zn}_{0.04}\text{Te}$ to improve lattice matching⁴¹ have been followed by striking experimental success not only in reducing dislocation densities at the interface, but also in reducing dislocation densities in the bulk substrate.⁴² This success in achieving lower dislocation densities for bulk $\text{Cd}_{0.96}\text{Zn}_{0.04}\text{Te}$ than for bulk CdTe must be understood as a macroscopic effect, because it cannot be explained by microscopic equilibrium properties, as we now discuss.

We find that equilibrium concentrations of vacancies and interstitials are not strongly affected by adding a small amount of an isoelectronic element substituting for either cation or anion, because the bond energies are only affected proportionally to the amount of the added element. For example, the bond energy E_b relative to a free-electron metal is only increased 1% in $\text{Cd}_{0.96}\text{Zn}_{0.04}\text{Te}$ over CdTe at 1365 K. In addition, this bond energy is only one contribution to enthalpies of native-defect formation. The enthalpy for vacancy formation, for example, also includes the energy of surface formation in a free-electron metal, ΔH_m , which is much larger than E_b . Similarly, the enthalpy for interstitial formation includes $I_0 \gg E_b$. Since the dominant defects are not neutral but charged, the ionization levels and the fundamental gap also play a major role in determining the total equilibrium defect concentrations.

Finally, for ternary and quaternary alloys, derivatives of the bond energy with respect to the different constituents enter the neutral-defect-formation enthalpies (examples are the terms containing E_b' in the defect-formation enthalpies listed for $\text{Hg}_{1-x}\text{Cd}_x\text{Te}$ in Sec. II). These terms enter because we do not use a local-bond approach, so a change in composition of the crystal changes the energy of all the bonds in the crystal. The effect of these terms is to require higher concentrations of some elements and lower concentrations of others in the external phase which is in equilibrium with an alloy of a given composition. Since cation and anion defect densities are determined by all the cation and anion species, large changes in bond strength as a function of composition, which will tend to favor the loss of one constituent while inhibiting the loss of another from the bonded lattice sites, will not necessarily lead to a decrease in equilibrium defect densities. A full equilibrium calculation must be done to determine the effect of changes in bond energies with composition on equilibrium point-defect densities. We will discuss this further, with reference to the effect on equilibrium defect densities of adding isovalent substituents to $\text{Hg}_{1-x}\text{Cd}_x\text{Te}$, in the next section.

These qualitative conclusions are in contradiction to published statements⁴³ on the effects of alloying due to changes in bond strength upon alloying. The statements

TABLE VII. Comparison of liquid, solid, and gas equilibrium at 1365 K.

	Native defects in equilibrium with:			
	V_C^{tot} (10^{17} cm^{-3})	I_c^{tot} (10^{17} cm^{-3})	V_A^{tot} (10^{17} cm^{-3})	I_A^{tot} (10^{17} cm^{-3})
Liquid	2.40	8.32	1.04	11.16
Solid	4.80	4.76	1.86	6.96
Gas	7.55	2.83	3.58	3.42

reflect a misunderstanding of the thermodynamics involved, as we show in the next section.

IV. RESULTS FOR $\text{Hg}_{0.8}\text{Cd}_{0.2}\text{Te}$

Figures 4 and 5 show the comparison between our results and Hall experiments^{24,44} done after quenching to 77 K from a higher-temperature anneal done at a specified Hg pressure. As for CdTe, it is necessary to know the Te pressure which would be in equilibrium with the solid at a given P_{Hg} . By using the same methods as before, we find the approximate relation for the pressure of monatomic Te:

$$P_{\text{Te}} = (1-x)(6.64 \times 10^{11} \text{ atm}^2) \\ \times \exp[-(3.09 \text{ eV})/(k_B T)]/P_{\text{Hg}}$$

Since cation vacancies can be determined by the Hg equilibrium without reference to Cd, and since cation interstitials are unimportant under the conditions of these experiments, it is not necessary to find the Cd pressure which would be in equilibrium under those conditions.

The agreement between calculated and observed hole concentrations in Figs. 4 and 5 is quite good, except that the charged vacancies begin to saturate at lower levels in the calculations than in the experiments. We believe this is due to our imperfect estimate of intrinsic carrier levels at elevated temperatures, as mentioned in Sec. II.

We have also tried assuming that both cation vacancy levels are extended, since no temperature dependence has been seen at low temperature, over a limited range of T , for the 10-meV second ionization level.²⁸ In this case, no choice of the first ionization level gives reasonable agreement with the Hall experiments. Therefore, we believe that the cation vacancy levels are localized, and will be

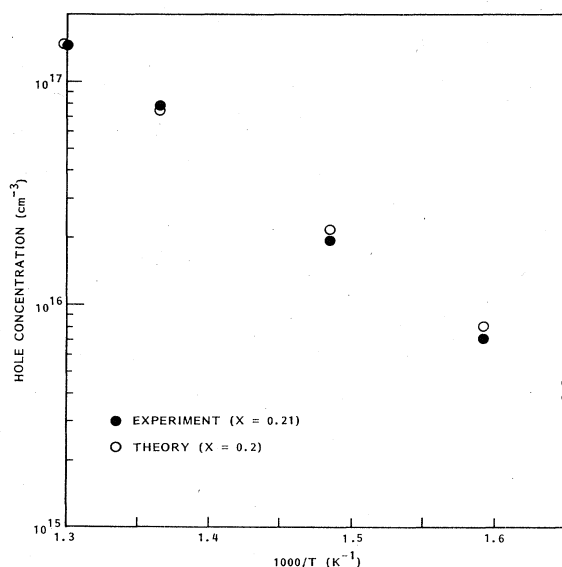


FIG. 4. $\text{Hg}_{1-x}\text{Cd}_x\text{Te}$: Hole concentration at 77 K after annealing at Hg vapor pressure. Both experimental (Ref. 44) and theoretical results are shown.

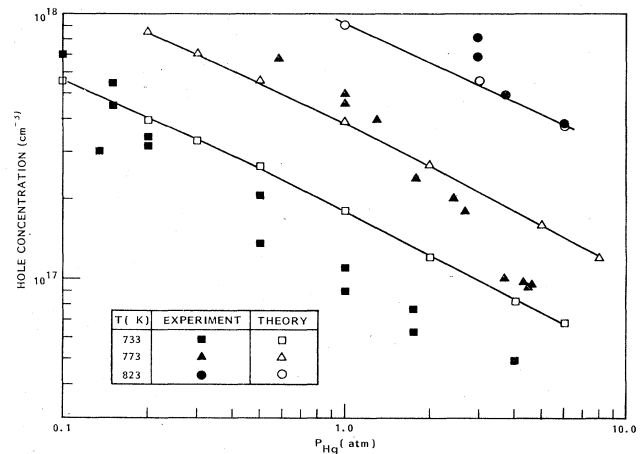


FIG. 5. $\text{Hg}_{0.8}\text{Cd}_{0.2}\text{Te}$: Experimental (Ref. 24) and theoretical hole concentration at 77 K after annealing at temperature T shown as a function of partial pressure of Hg. Considerable scatter exists in the experimental data.

seen to vary with temperature relative to the valence-band edge. At the higher Hg pressures, concentrations of neutral cation vacancies are less than concentrations of neutral anion vacancies. However, due to the favorable ionization levels, charged-cation vacancies dominate in all cases. In order to separate out the effects of the external phase from inherent properties of the alloy, we show in Fig. 6 the concentrations of charged native defects expected for the solid in equilibrium with no external phase

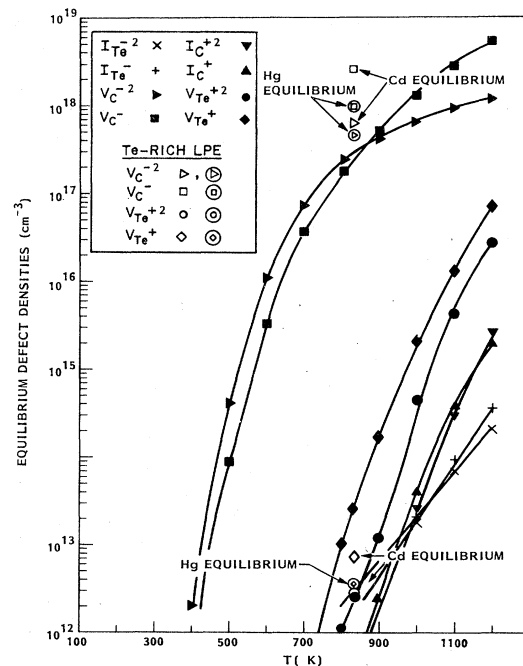


FIG. 6. $\text{Hg}_{0.8}\text{Cd}_{0.2}\text{Te}$: Solid with no external phase. Points showing theoretical calculations under conditions appropriate to liquid-phase-epitaxial growth from Te-rich solutions are also shown.

available. In contrast to CdTe, $\text{Hg}_{0.8}\text{Cd}_{0.2}\text{Te}$ is seen to be not strongly compensated, but dominated by charged-cation vacancies at all temperatures. At temperatures above 700 K, the Fermi level begins to be determined by these charged defects, so that they saturate, although the neutral defect concentrations continue to increase. As in Fig. 4 and 5, we have used $I_0 = 1.65$ eV. If we were to use $I_0 = 1$ eV for cation interstitials, Hg interstitial concentrations would be increased to 2.5×10^{15} at 800 K. If this lower value of I_0 for cation interstitials is correct in $\text{Hg}_{0.8}\text{Cd}_{0.2}\text{Te}$, then frozen-in concentrations of Hg interstitials or complexes may be important in contributing midgap tunneling levels, as suggested by recent experiments.⁴⁵

Figure 6 also includes the charged-defect densities expected in equilibrium for Te-rich liquid-phase epitaxy at 825 K, using a solution of $\text{Hg}_{0.23325}\text{Cd}_{0.01675}\text{Te}_{0.75}$.⁴⁶ Note that the ratio of Hg to Cd is much higher in the liquid than in the alloy in equilibrium with the liquid. This is due to the greater volatility of Hg, and, in particular, to the E'_b term in the enthalpy for reactions involving the movement of a cation between the crystal and the liquid, which favors loss of Hg to the liquid and retention of Cd in the alloy. At the high concentrations of cation vacancies shown in the figure, it may be expected that the ionization levels become less favorable due to overlap (this effect has already been seen at low temperature²⁸), so that these defect concentrations should actually be somewhat reduced.

We show the charged-defect concentrations calculated by assuming the cation vacancies are in equilibrium with both the Cd and the Hg in the external phase. If we have correctly estimated the changes in free energy for both Cd and Hg leaving the crystal, these defect concentrations should be identical. Considering the rough approximations made, the agreement is quite good.

Since the addition of a small amount of another iso-valent cation or anion cannot change E_b dramatically, and since E_b is not the major contributor to enthalpies of defect formation in any case, adding small amounts of other elements is not expected to reduce native-defect concentrations dramatically in Hg-rich $\text{Hg}_{1-x}\text{Cd}_x\text{Te}$. The larger changes in bond energy for the Hg-Te bond in different alloys which are calculated using the local-bond picture² correspond more nearly to our E'_b terms than to the small changes in E_b . Since a stabilization of one element in the alloy by a favorable E'_b is always accompanied by a destabilization of the other element, it is not obvious whether a high sensitivity of the bond strength to relative composition, i.e., a high E_b , is desirable or not. The only obvious effect of the E'_b terms will be to determine the relative composition of the external phase which can be in equilibrium with an alloy of a given composition; the effect on equilibrium native-defect concentrations cannot be predicted on the basis of bond stabilization or destabilization alone, without a full thermodynamic calculation. Of course, dramatic changes in macroscopic properties of ternary alloys, due to nonequilibrium phenomena such as a change in defect pinning, or macroscopic phenomena such as improved lattice matching, are still quite possible.

We conclude by discussing the cation-vacancy ionization levels chosen here. For $\text{Hg}_{0.8}\text{Cd}_{0.2}\text{Te}$, it seems that the first ionization level must be chosen below the valence-band edge and the second only about 10 meV above it for $T \approx 50$ K to give good agreement with experiment. With one exception,²⁸ this is not in agreement with the general belief, which places the *first* level 10–15 meV above the band. The second level is assumed to provide trap states to agree with experiments on tunneling currents. However, the charge state of the (10–15)-meV level has never been identified unambiguously as a singly ionized state.

Our calculations lend further credence to Vydyanath's arguments⁴⁵ that vacancy levels do not provide recombination centers for tunneling. It would be most interesting and useful to verify the vacancy ionization levels, and, in particular, the level we find below the valence-band edge, and also to identify the tunneling centers in $\text{Hg}_{0.8}\text{Cd}_{0.2}\text{Te}$.

V. CONCLUSIONS

We have used the dielectric theory of Phillips and Van Vechten, suitably modified, to study the defect chemistry of $\text{Hg}_{1-x}\text{Cd}_x\text{Te}$. We achieve reasonable agreement with Hall experiments done at high temperatures and at 77 K on quenched samples, by using experimentally identified low-temperature ionization levels, and assuming that all the charged states of native defects, with the exception of cation interstitials in Hg-rich $\text{Hg}_{1-x}\text{Cd}_x\text{Te}$, are highly localized.

For both CdTe and Hg-rich $\text{Hg}_{1-x}\text{Cd}_x\text{Te}$, favorable ionization levels for native defects cause large equilibrium concentrations of charged defects. CdTe is highly compensated at temperatures near the maximum melting point, with a net deviation from stoichiometry ($\approx 10^{17}/\text{cm}^3$ excess Te) resulting from the sum of larger concentrations of both donor and acceptor defects. $\text{Hg}_{0.8}\text{Cd}_{0.2}\text{Te}$ is dominated by charged-cation vacancies, although cation interstitials may be sufficiently numerous to provide midgap tunneling levels. Under the assumptions made in this paper, the cation vacancies do not provide the midgap levels. The greater stability of less metallic, more-Cd-rich $\text{Hg}_{1-x}\text{Cd}_x\text{Te}$, as well as the greater volatility of Hg, results in a preferential loss of Hg, which must be balanced by a larger $[\text{Hg}]/[\text{Cd}]$ ratio in the external phase than in the alloy at equilibrium. It is shown that the addition of small amounts of other cations or anions should not have a dramatic effect on equilibrium densities of native defects in these materials, although crystal quality may be dramatically affected by changes in nonequilibrium and macroscopic phenomena involved in the formation of extended defects.

ACKNOWLEDGMENTS

We thank Dr. James Van Vechten for several discussions and Dr. H. R. Vydyanath for detailed conversations

and guidance to the literature of defect studies on the $\text{Hg}_{1-x}\text{Cd}_x\text{Te}$ system. We also thank Dr. Soo Shin and Dr. C. Jones for sharing their experimental results with us. One of us (R.R.) thanks Dr. James Phillips for discussion in an early phase of this work. The other one of us (C.M.P.) thanks Dr. M. Schlüter for a helpful discussion

on the Jahn-Teller effect. The work was supported by the U.S. Department of Defense Advanced Research Program Agency (DARPA) under Contract No. DAAH01-80-C0493 while the authors were at Riverside Research Institute. The paper was completed under Lockheed Internal Research Funds.

*Present address: Department of Physics, Wayne State University, Detroit, MI 48202.

†To whom reprint requests should be addressed.

- ¹J. A. Van Vechten, in *Handbook in Semiconductors*, edited by T. S. Moss (North-Holland, Amsterdam, 1980), Vol. 3, Chap. 1.
- ²W. A. Harrison, *Electronic Structure* (Freeman, San Francisco, 1980).
- ³J. C. Phillips and J. A. Van Vechten, *Phys. Rev. Lett.* **30**, 220 (1973).
- ⁴J. A. Van Vechten, *J. Electrochem. Soc.* **122**, 419 (1975).
- ⁵J. A. Van Vechten and C. D. Thurmond, *Phys. Rev. B* **14**, 3539 (1976).
- ⁶V. Heine and C. H. Henry, *Phys. Rev. B* **11**, 3795 (1975).
- ⁷H. H. Woodbury and R. B. Hall, *Phys. Rev.* **157**, 641 (1967).
- ⁸H. B. Huntington and Frederick Seitz, *Phys. Rev.* **61**, 315 (1942).
- ⁹H. B. Huntington, *Phys. Rev.* **91**, 1092 (1953).
- ¹⁰J. A. Van Vechten, *J. Electrochem. Soc.* **122**, 423 (1975).
- ¹¹J. A. Van Vechten and J. C. Phillips, *Phys. Rev. B* **2**, 2160 (1970).
- ¹²G. Simons and A. N. Bloch, *Phys. Rev.* **7**, 2754 (1973); G. Simons, *J. Chem. Phys.* **55**, 756 (1971). See also J. St. Johns and A. N. Bloch, *Phys. Rev. Lett.* **33**, 1095 (1974).
- ¹³J. A. Van Vechten, *Phys. Rev.* **182**, 891 (1969).
- ¹⁴J. A. Van Vechten, *Phys. Rev. B* **7**, 1479 (1973).
- ¹⁵D. R. Penn, *Phys. Rev.* **128**, 2093 (1962).
- ¹⁶A. Moritani, K. Taniguchi, C. Hamaguchi, and J. Nakai, *J. Phys. Soc. Jpn.* **34**, 79 (1973).
- ¹⁷J. L. Schmit and E. L. Stelzer, *J. Appl. Phys.* **40**, 4865 (1969).
- ¹⁸H. Arwi and D. E. Aspnes (unpublished). Other work on optical features in the E_2 region for $\text{Hg}_{1-x}\text{Cd}_x\text{Te}$ includes A. Rodzik and A. Kisiel, *J. Phys. C* **16**, 203 (1983), and D. K. Chadi, John P. Walter, Marvin Cohen, Y. Petroff, and M. Balkanski, *Phys. Rev. B* **5**, 3058 (1972).
- ¹⁹D. E. Aspnes (private communication).
- ²⁰J. A. Van Vechten, *Phys. Rev.* **187**, 1007 (1969).
- ²¹R. Ludeke, *J. Appl. Phys.* **39**, 4028 (1968).
- ²²C. Verie and J. Ayas, *Appl. Phys. Lett.* **10**, 241 (1967).
- ²³V. Heine and J. A. Van Vechten, *Phys. Rev. B* **13**, 1622 (1976).
- ²⁴H. R. Vydyanath, *J. Electrochem. Soc.* **128**, 2609 (1981).
- ²⁵J. Schmit and A. A. Lucas, *Collect. Phen.* **1**, 127 (1973).
- ²⁶R. M. Martin, *Phys. Rev. B* **1**, 4005 (1970).
- ²⁷S. S. Chern, H. R. Vydyanath, and F. A. Kroger, *J. Solid State Chem.* **14**, 33 (1975).
- ²⁸Colin Jones (private communication).
- ²⁹P. W. Davis and T. S. Shilliday, *Phys. Rev.* **118**, 1020 (1960).
- ³⁰L. K. S. Ladd, *Infrared Phys.* **6**, 145 (1966).
- ³¹K. K. Kanazawa and F. C. Brown, *Phys. Rev.* **135**, A1757 (1964).
- ³²M. Weiler, in *Semiconductors and Semimetals*, edited by R. K. Willardson and Albert C. Beer (Academic, New York, 1981), Vol. 16, Chap. 3.
- ³³A. V. Savitskii, [*Sov. Phys.—Semicond.* **6**, 1760 (1973)].
- ³⁴R. Dornhaus and G. Nimtz, *Narrow Gap Semiconductors*, Vol. 98 of *Springer Tracts in Modern Physics* (Springer, Berlin, 1983), Chap. 2.
- ³⁵J. Alper and G. A. Saunders, *J. Phys. Chem. Solids* **28**, 1637 (1967).
- ³⁶R. E. Halsted *et al.*, *J. Phys. Chem. Solids* **22**, 109 (1961).
- ³⁷*Metals Handbook* (American Society of Metals, Cleveland, 1948).
- ³⁸H. R. Vydyanath (private communication).
- ³⁹A. S. Jordan, *Metall. Trans.* **1**, 239 (1970).
- ⁴⁰K. Zanio, in *Semiconductors and Semimetals*, edited by D. Willardson and A. C. Beer (Academic, New York, 1978), Vol. 13.
- ⁴¹The suggestions for incorporation of Zn are quite old. See, for example, Lockheed Palo Alto Report No. 894343, Dec. 1965 (unpublished).
- ⁴²S. L. Bell and S. Sen, in Extended Abstracts of the 1984 U.S. Workshop on the Physics and Chemistry of HgCdTe (unpublished).
- ⁴³A. Sher, An-Ban Chen, W. E. Spicer, and C. K. Shih, in Extended Abstracts of the 1984 U.S. Workshop on the Physics and Chemistry of HgCdTe (unpublished).
- ⁴⁴S. Shin and M. Khoshnevisan, in Extended Abstracts of the 1984 U.S. Workshop on the Physics and Chemistry of HgCdTe (unpublished); S. H. Shin, M. Khoshnevisan, C. Morgan-Pond, and R. Raghavan (unpublished).
- ⁴⁵H. R. Vydyanath (private communication).
- ⁴⁶J. S. Mroczkowski and H. R. Vydyanath, *J. Electrochem. Soc.* **128**, 655 (1981).